

Supporting Information

for

Isorecticular Zirconium-Based Metal-Organic Frameworks: Discovering Mechanical Trends and Elastic Anomalies Controlling Chemical Structure Stability

M. R. Ryder,¹ B. Civalleri,² and J. C. Tan^{1*}

¹Department of Engineering Science, University of Oxford,

²Department of Chemistry, University of Turin

*Correspondence to: jin-chong.tan@eng.ox.ac.uk

Table of Contents

1.	<i>Ab Initio</i> Quantum Mechanical DFT Calculations	3-4
2.	DFT Optimized Lattice Parameters (Table S2)	5
3.	Difference from Previously Published DFT Values	6
4.	Young's Modulus 3-D Plots for MIL-140(A-D)	7
5.	Shear Modulus 3-D Plots for MIL-140(A-D)	8-9
6.	Poisson's Ratio 3-D Plots for MIL-140(A-D)	10-11
7.	Poisson's Ratio Data (Table S3)	12
8.	References	13

1. *Ab Initio* Quantum Mechanical DFT Calculations

Density functional theory (DFT) calculations were carried out at the B3LYP level of theory¹ and performed with the periodic ab initio code CRYSTAL09.² Crystalline orbitals were represented as linear combinations of Bloch functions (BF), and were evaluated over a regular three-dimensional (3D) mesh in reciprocal space. Each BF was constructed from local atomic orbitals (AOs), which are linear combinations (with constant coefficients) of Gaussian-type functions (GTFs). Each GTF is the result of a Gaussian multiplied by a solid spherical harmonic.

All electron basis sets were used for Zr³, O⁴, C⁵ and H⁶ atoms. The adopted basis sets contain 1016, 1280, 1432 and 1712 basis functions for MIL-140A, MIL-140B, MIL-140C and MIL-140D, respectively.

A full relaxation of both lattice parameters and atomic coordinates was allowed. The geometry optimisation at constant symmetry was performed by means of a quasi-Newtonian algorithm in which the quadratic step (BFGS Hessian updating scheme) is combined with a linear one (parabolic fit) as proposed by Schlegel.⁷ Convergence was tested on the root mean square (RMS) and the absolute value of the largest component of the gradients and the estimated displacements. The threshold for the maximum and RMS gradient, and the maximum and RMS atomic displacement of all atoms was set to 1.5×10^{-4} , 1.0×10^{-4} , 3.0×10^{-4} and 2.0×10^{-4} a.u., respectively. The optimisation was considered to have completed when all four conditions were simultaneously satisfied.

The elastic constants are obtained from the optimised structure by first calculating the single-point self-consistent-field (SCF) energy of the optimised structure and then calculating the six sets of required strains (due to MIL-140 being monoclinic). For each unique strain (0.01) the structure is deformed and the new symmetry elements are determined. This occurs for multiple strain steps to increase the accuracy of the resultant gradient. For each deformed structure the atomic coordinates are relaxed and optimised as above. Another SCF energy calculation is then performed at each optimised deformation and the energy gradient is fitted with singular-value-decomposition routines and the second derivatives are determined numerically. This then allows for the elastic constants to be computed.⁸

The robustness of the results were confirmed through multiple methods, first by redoing the calculations for MIL-140A using the new version of the code, CRYSTAL14.⁹ We also ran the calculations for MIL-140A using a very large basis set (1264 Basis functions – 25% larger) to reduce any basis set superposition error (BSSE) and finally increased the number of deformation points beyond the default to 5. The values from the checks are reported in Table S1.

TABLE S1 Elastic properties of MIL-140A

Elastic Property		CRYSTAL09 Results reported in the paper	CRYSTAL14 Otherwise as the reported work	CRYSTAL14 Larger Basis Set Used	CRYSTAL14 Large Basis Set and Multiple Deformation Points
Young's Modulus (GPa)	E_{\max}	142.0	142.7	137.7	137.9
	E_{\min}	11.3	11.1	12.0	12.1
	$A_E = E_{\max}/E_{\min}$	12.6	12.8	11.5	11.4
Shear Modulus (GPa)	G_{\max}	36.9	36.8	35.6	35.8
	G_{\min}	3.2	3.1	3.4	3.4
	$A_G = G_{\max}/G_{\min}$	11.5	11.8	10.5	10.5
Linear Compressibility (TPa ⁻¹)	β_{\max}	27.8	27.9	25.8	25.4
	β_{\min}	-3.0	-3.0	-2.3	-2.1
Poisson's Ratio	ν_{\max}	1.11	1.11	1.06	1.06
	ν_{\min}	-0.13	-0.13	-0.08	-0.08
Ledbetter Anisotropy	A^*	12.5	12.6	11.5	11.2

It is clear that using CRYSTAL09 or CRYSTAL14 has no effect on values used for this work. It is also evident that using 5 points on the deformation gradient instead of 3 has no effect beyond numerical noise. The use of a significantly difference basis set has only a small effect that would always be expected. We can therefore conclude that the values used in this work are robust for the level of theory used.

2. DFT Optimized Lattice Parameters (Table S2)

Summarized below are the comparisons of lattice parameters calculated from DFT (for ideal crystalline structures) versus experimental values reported in literature.¹⁰

MIL-140A					
Method	Lattice parameters (Å)			Monoclinic Angle	Volume (Å ³)
	<i>a</i>	<i>b</i>	<i>c</i>	β	
Literature	24.4243	11.1795	7.8022	103.861	2068.36
B3LYP	24.7627	11.2756	7.9779	102.482	2175.00
<ul style="list-style-type: none"> Average error in lattice parameters (including angle): 1.49% 					

MIL-140B					
Method	Lattice parameters (Å)			Monoclinic Angle	Volume (Å ³)
	<i>a</i>	<i>b</i>	<i>c</i>	β	
Literature	28.1582	13.4675	7.8890	93.43	2986.31
B3LYP	28.1881	13.4869	8.0237	94.55	3040.73
<ul style="list-style-type: none"> Average error in lattice parameters (including angle): 0.78% 					

MIL-140C					
Method	Lattice parameters (Å)			Monoclinic Angle	Volume (Å ³)
	<i>a</i>	<i>b</i>	<i>c</i>	β	
Literature	31.8931	15.6099	7.9348	84.83	3934.25
B3LYP	31.7993	15.6266	8.0147	85.99	3972.96
<ul style="list-style-type: none"> Average error in lattice parameters (including angle): 0.54% 					

MIL-140D					
Method	Lattice parameters (Å)			Monoclinic Angle	Volume (Å ³)
	<i>a</i>	<i>b</i>	<i>c</i>	β	
Literature	34.8613	17.4795	7.8598	90.27	4789.38
B3LYP	35.4850	17.5900	7.9771	95.32	4957.72
<ul style="list-style-type: none"> Average error in lattice parameters (including angle): 2.37% The increased error for MIL-140D is due to the Literature CIF file not containing the disordered Cl atoms. 					

3. Difference from Previously Published DFT Values

The reason our results for MIL-140A differ from values already published¹¹ is due to the already published results likely having been performed with a bugged version of Crystal09 (version 2.0). This problem was removed in a patch fix for Crystal09 (version 2.01) and is no longer present in the latest edition of the code.

The main changes in the fix (2.01) was the way the minimal set of deformations needed to compute the elastic tensor is defined. Also, they fixed a bug in the transformation of the strain derivatives from primitive to conventional unit cells. This was due to the transformation being done in an incorrect way in version 2.0. The result was that it worked for some lattices but not for non-orthogonal non-primitive lattices, including most monoclinic space groups and hexagonal/rhombohedral lattices as well. There was also a misprinting in the elastic tensor for triclinic crystals which was fixed.

Another obvious sign that the 2.0 version results are incorrect is that they give a lower maximum value for the Young's modulus, for the 'reinforced' MIL-140A than is reported for the flexible non-reinforced 'wine-rack' frameworks.

The matrix below is what we obtained for MIL-140A using Crystal09 (2.01):

$$C_{\text{Voigt}} = \begin{pmatrix} 93.956 & 42.703 & 29.575 & 0 & -4.008 & 0 \\ & 163.02 & 17.443 & 0 & 0.27 & 0 \\ & & 52.706 & 0 & -10.384 & 0 \\ & & & 3.194 & 0 & 0.099 \\ & & & & 9.05 & 0 \\ & & & & & 27.424 \end{pmatrix}$$

The matrix below is what we obtained for MIL-140A using Crystal09 (2.0):

$$C_{\text{Voigt}} = \begin{pmatrix} 46.553 & 21.429 & 29.372 & 0 & 1.296 & 0 \\ & 81.483 & 17.352 & 0 & 2.050 & 0 \\ & & 52.881 & 0 & 0.726 & 0 \\ & & & 1.637 & 0 & 0.140 \\ & & & & 3.355 & 0 \\ & & & & & 13.429 \end{pmatrix}$$

The values obtained using the bugged 2.0 version of Crystal09 give results more consistent with the published values for MIL-140A.

However, we would like to highlight that the previously reported values are incorrect due to a bug in the Crystal09 code that now has been fixed in CRYSTAL14, and not due to any mistake by the authors of ref. [11].

4. Young's Modulus 3-D Plots for MIL-140(A-D)

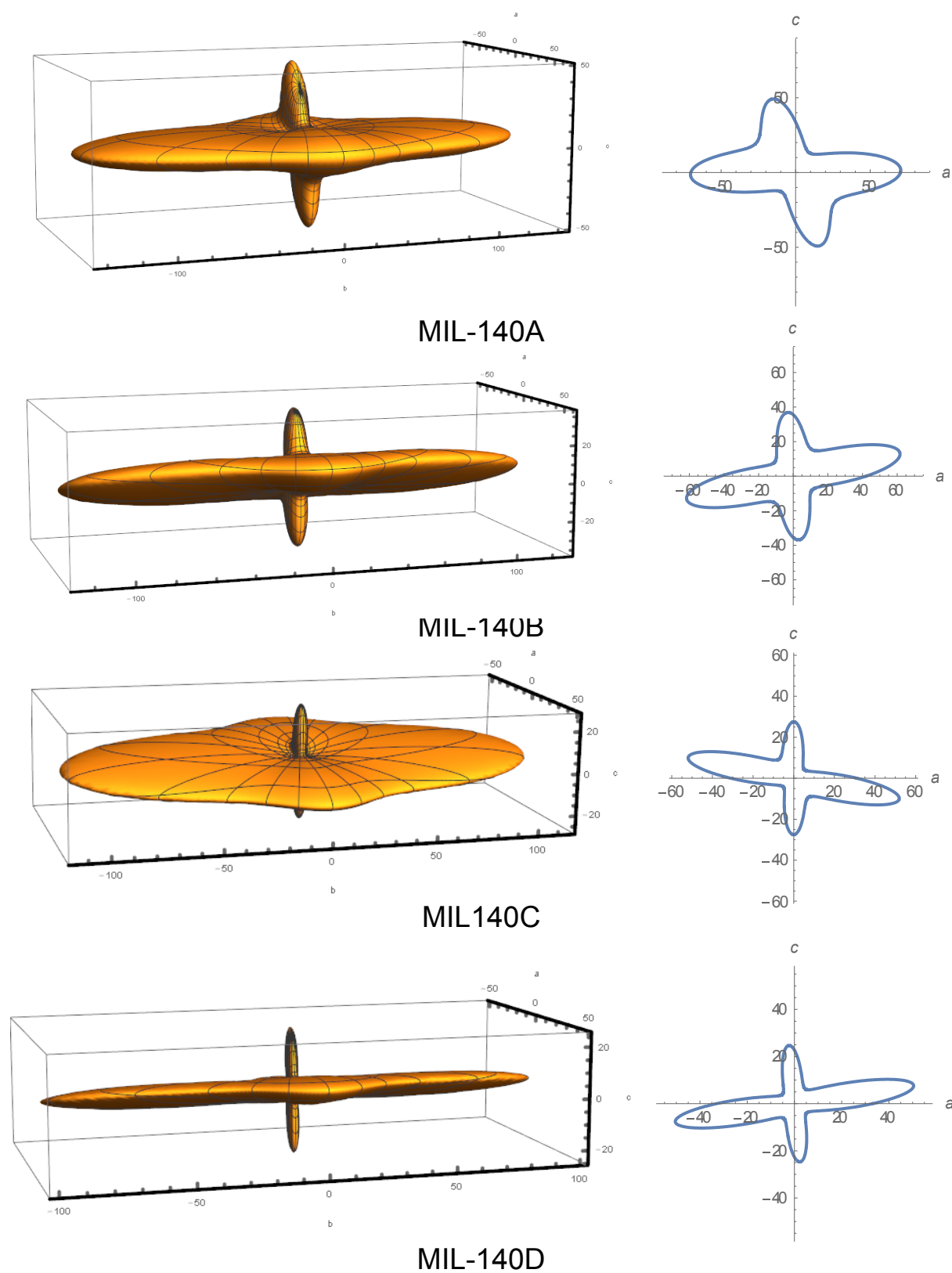
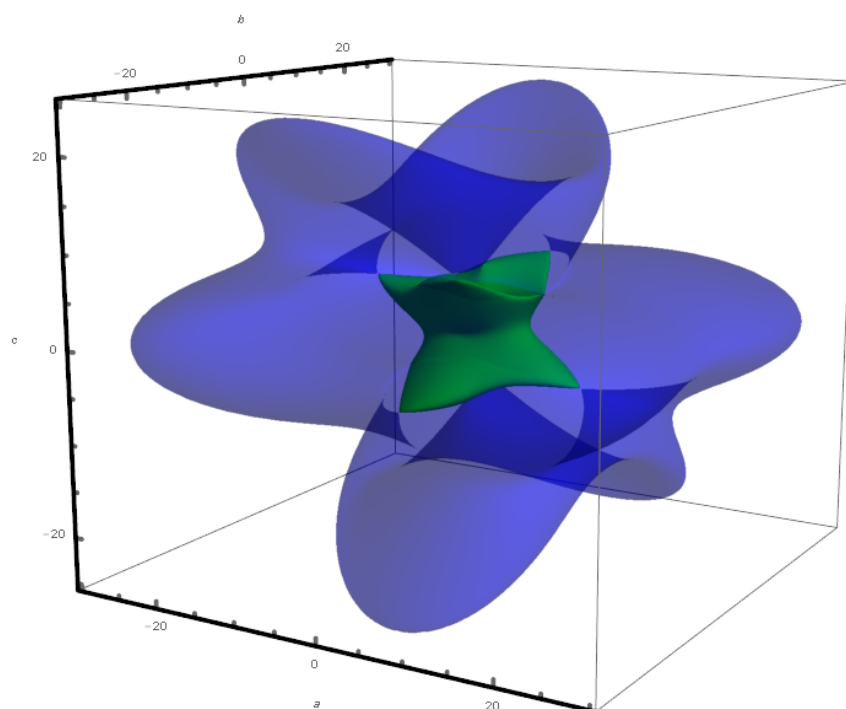
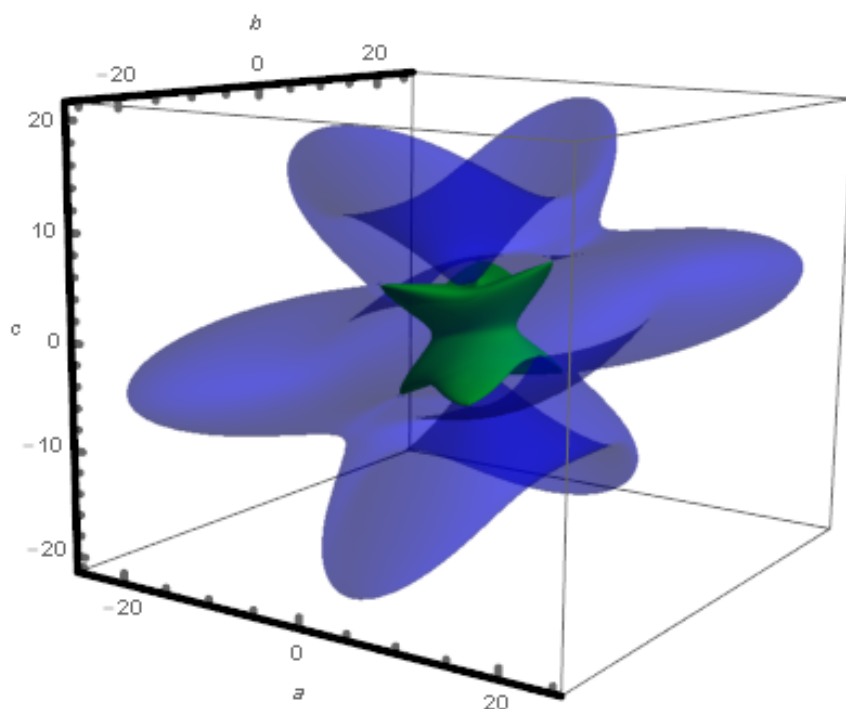


Fig. S1: (Left panel) 3-D Young's modulus representation surfaces $E(\theta, \varphi)$ of MIL-140(A-D). (Right panel) 2-D projections down the b -axis.

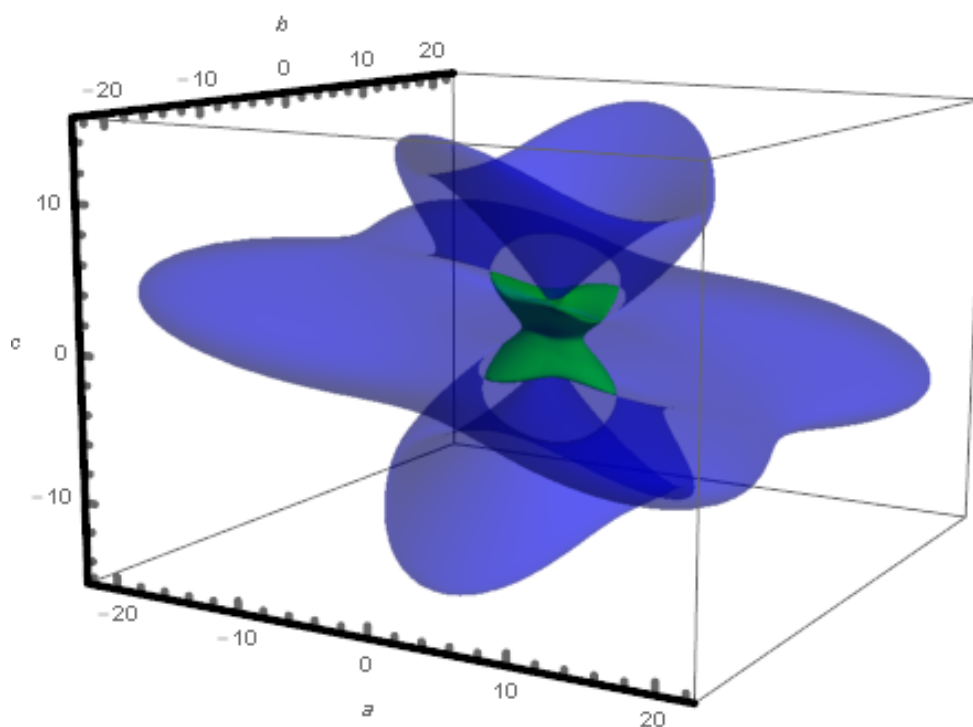
5. Shear Modulus 3-D Plots for MIL-140(A-D)



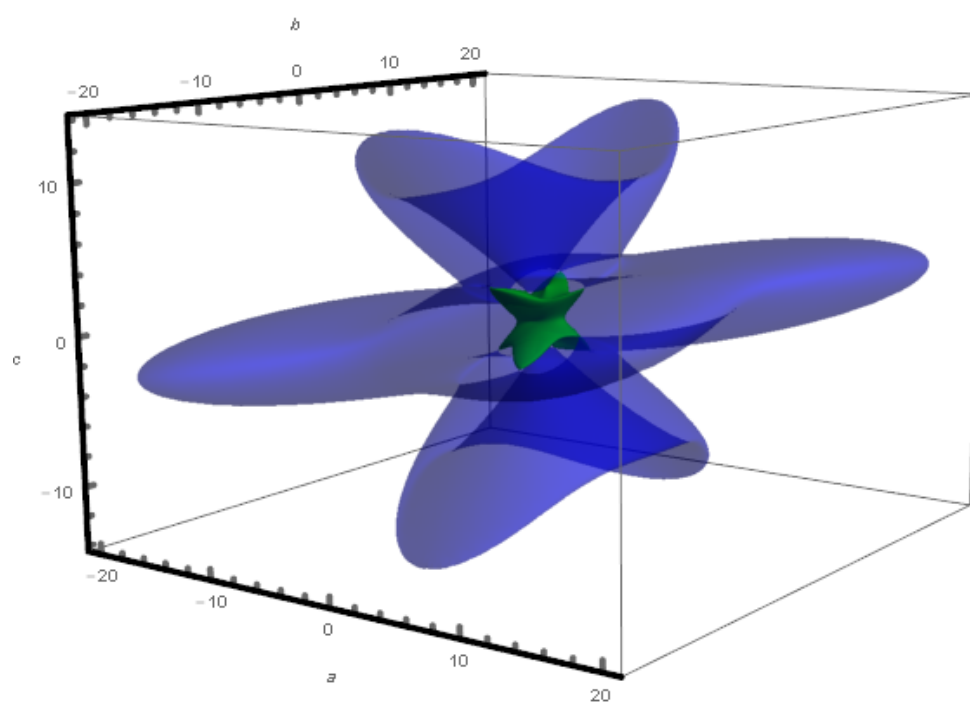
MIL-140A



MIL-140B



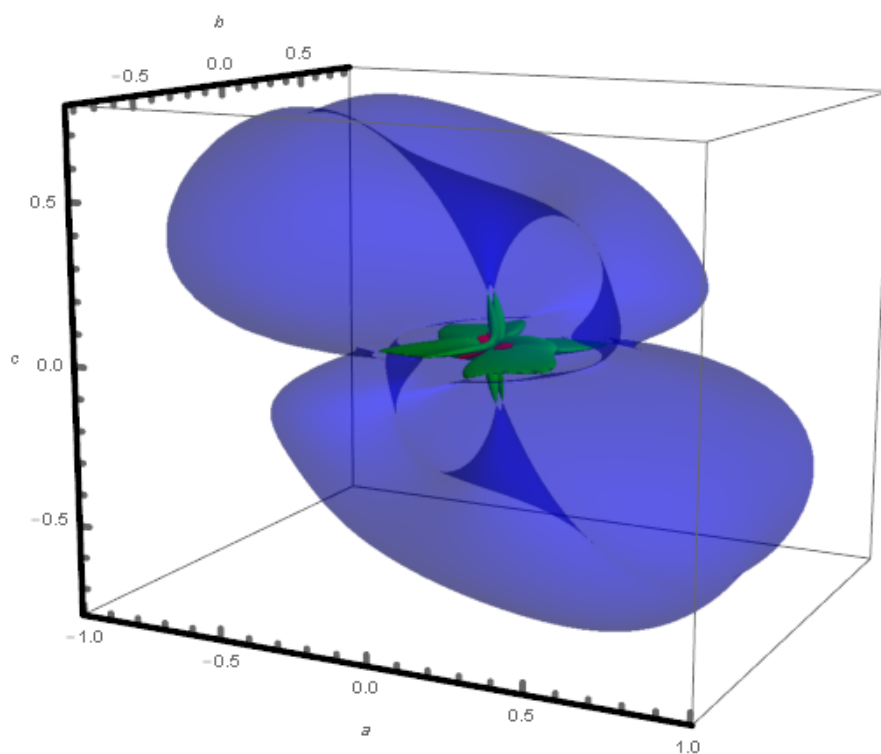
MIL-140C



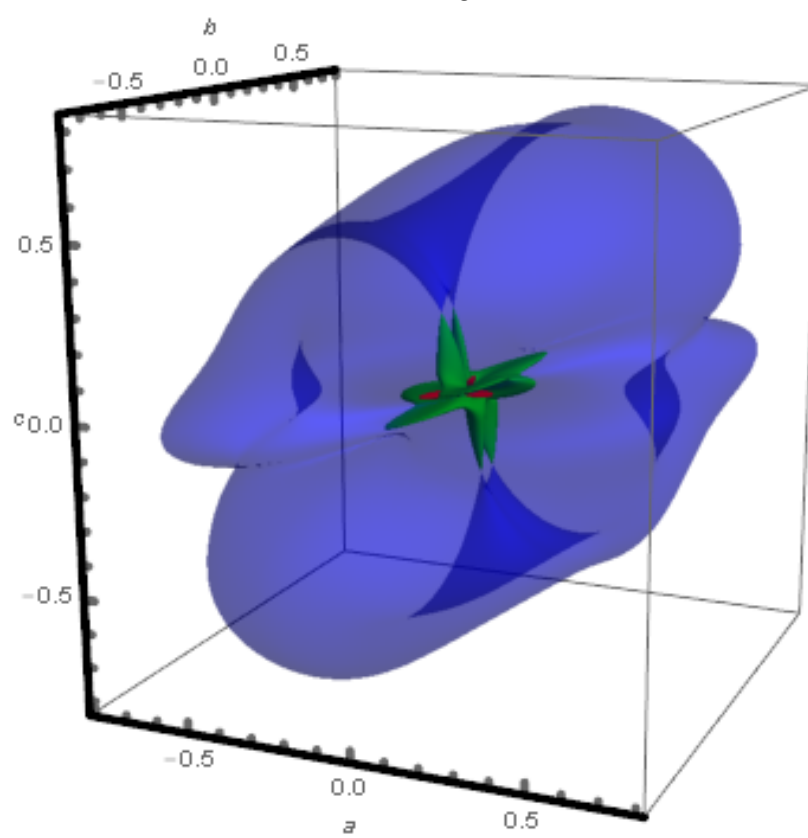
MIL-140D

Fig. S2: 3-D shear modulus representation surface $G(\theta, \varphi, \chi)$ of MIL-140(A-D). Color coding used: blue and green represent the maximum and minimum moduli, respectively.

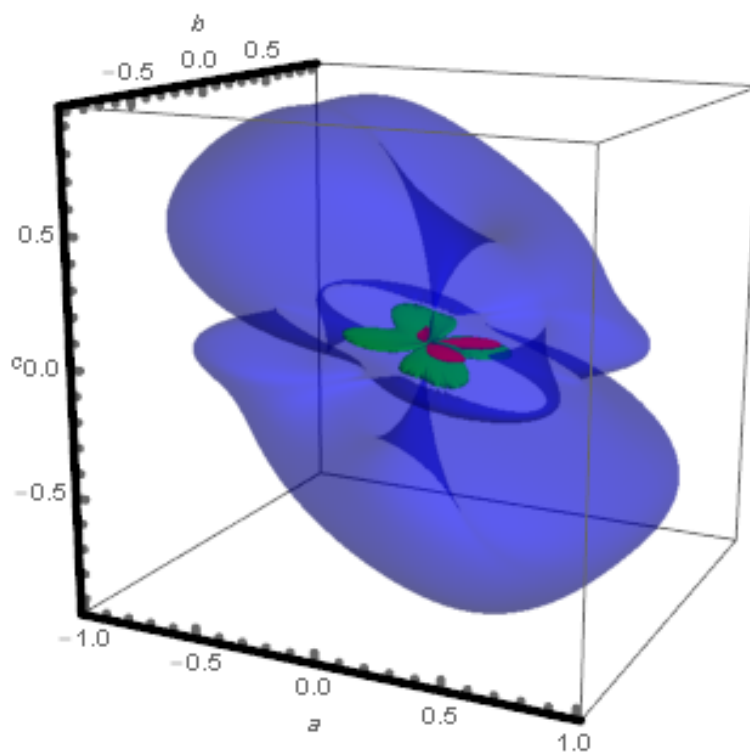
6. Poisson's Ratio 3-D Plots for MIL-140(A-D)



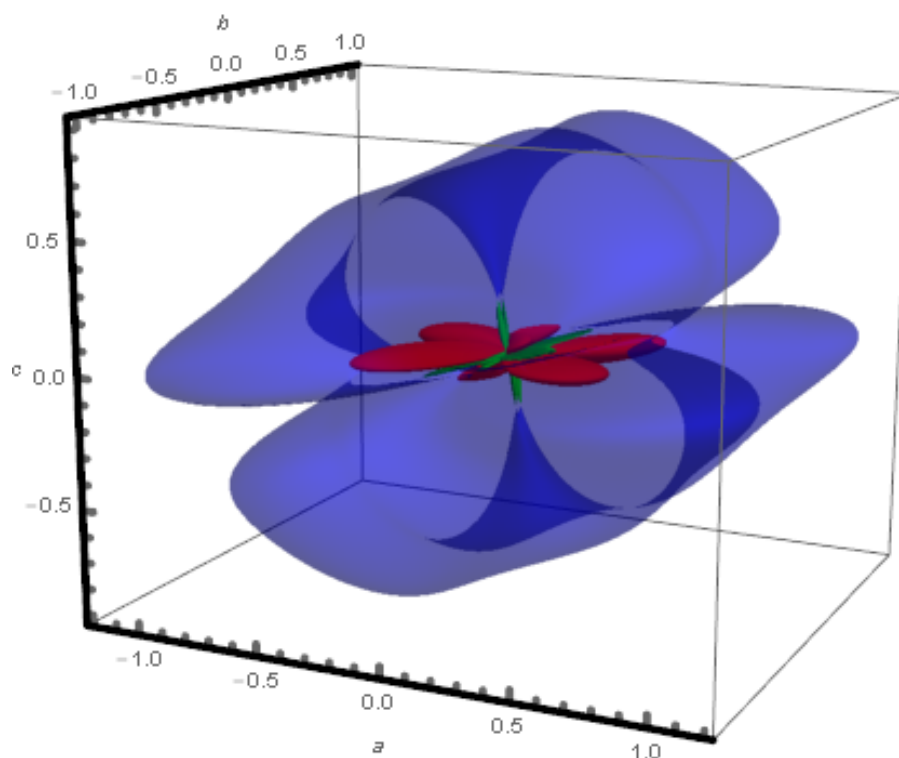
MIL-140A



MIL-140B



MIL-140C



MIL-140D

Fig. S3: 3-D Poisson's ratio representation surface $v(\theta, \varphi, \chi)$ of MIL-140(A-D). Blue surface represents the maximum Poisson's ratio and green and red surfaces denote the positive and negative minimum Poisson's ratios, respectively.

7. Poisson's Ratio Data (Table S3)

Material	A^*	ν_{\max}	ν_{\max} load direction	ν_{\max} transverse direction	ν_{\min}	ν_{\min} load direction	ν_{\min} transverse direction	Reference
Augite	1.59	0.53	[-3 0 4]	[4 0 3]	-0.10	[4 0 9]	[0 1 0]	[12]
Lanthanum pentaphosphate	1.73	0.48	[5 -7 10]	[11 34 18]	0.02	[0 1 0]	[-37 0 14]	[12]
Jadeite	1.79	0.45	[29 14 24]	[25 2 -31]	0.13	[-20 0 3]	[3 0 20]	[12]
Aegirite-Augite	1.94	0.64	[3 0 -2]	[0 1 0]	-0.01	[21 0 34]	[0 1 0]	[12]
Spodumene	1.95	0.52	[-23 0 33]	[33 0 23]	0.09	[-8 0 1]	[1 0 8]	[12]
Coesite	2.83	0.73	[-6 0 19]	[19 0 6]	-0.11	[-11 0 39]	[0 1 0]	[12]
BiVO_4	2.89	0.68	[-3 0 13]	[13 0 3]	-0.03	[0 1 0]	[39 0 8]	[12]
Albite	2.96	0.66	[-20 -22 27]	[5 29 27]	0.01	[7 0 19]	[0 1 0]	[12]
$\text{K}_2\text{Co}(\text{CN})_6$	3.08	0.62	[3 0 40]	[40 0 -3]	-0.36	[23 0 33]	[0 1 0]	[12]
Betaine phosphate	3.19	0.80	[-7 4 6]	[27 26 14]	-0.04	[0 1 0]	[37 0 16]	[12]
ZrO_2	3.23	0.82	[0 1 0]	[26 0 31]	-0.04	[-11 14 9]	[-22 -28 19]	[12]
Hyalophane	4.36	0.74	[-6 0 19]	[19 0 6]	-0.03	[0 1 0]	[1 0 -40]	[12]
Biphenyl	4.98	1.07	[10 0 39]	[0 1 0]	-0.26	[7 0 39]	[39 0 -7]	[12]
CsDSeO_3	7.11	1.03	[6 -17 8]	[-31 1 26]	-0.30	[39 0 10]	[10 0 -39]	[12]
$\text{C}_{16}\text{F}_{26}\text{H}_4$	7.70	1.18	[27 27 11]	[2 3 -13]	-0.50	[-23 31 -11]	[33 23 -3]	[12]
Durene	9.71	0.88	[0 1 0]	[38 0 11]	-0.12	[3 0 13]	[13 0 -3]	[12]
A-TCNB	32.37	1.88	[37 8 -12]	[1 15 13]	-1.05	[37 7 -14]	[15 -25 28]	[12]
CsH_2PO_4	53.46	2.71	[10 -33 21]	[39 11 -1]	-1.93	[-10 17 -4]	[35 20 -4]	[12]
LaNbO_4	57.26	3.96	[0 1 0]	[21 0 -34]	-3.01	[1 -40 -1]	[34 1 21]	[12]
ZIF-8	1.37	0.57	[1 0 1]	[1 0 -1]	0.33	[1 0 1]	[0 1 0]	[13]
MOF-5	2.10	0.67	[1 0 1]	[1 0 -1]	0.03	[1 0 1]	[0 1 0]	[14]
MIL-140A	12.50	1.11	[79 39 -46]	[24 50 83]	-0.13	[-73 65 -22]	[-61 -45 65]	This Work
MIL-140B	13.60	0.98	[52 -49 70]	[51 -48 -71]	-0.15	[74 -67 8]	[31 45 84]	This Work
MIL-140C	23.16	1.16	[70 44 -56]	[38 43 82]	-0.28	[-80 -60 4]	[34 -50 -80]	This Work
MIL-140D	36.89	1.37	[-81 59 -3]	[-46 -60 66]	-0.61	[83 -55 4]	[34 56 75]	This Work

8. References

1. Becke, A. D., Density-Functional Thermochemistry .3. The Role of Exact Exchange. *J Chem Phys* **1993**, *98* (7), 5648-5652.
2. Dovesi, R.; Saunders, V. R.; Roetti, C.; Orlando, R.; Zicovich-Wilson, C. M.; Pascale, F.; Civalleri, B.; Doll, K.; Harrison, N. M.; Bush, I. J.; D'Arco, P.; Llunell, M. *CRYSTAL09 User's Manual, University of Torino, Torino, 2009*.
3. Dovesi, R., http://www.crystal.unito.it/Basis_Sets/zirconium.html. *Unpublished*.
4. Bredow, T.; Jug, K.; Evarestov, R. A., Electronic and magnetic structure of ScMnO₃. *physica status solidi (b)* **2006**, *243* (2), R10-R12.
5. Spackman, M. A.; Mitchell, A. S., Basis set choice and basis set superposition error (BSSE) in periodic Hartree-Fock calculations on molecular crystals. *Phys Chem Chem Phys* **2001**, *3* (8), 1518-1523.
6. Corno, M.; Busco, C.; Civalleri, B.; Ugliengo, P., Periodic ab initio study of structural and vibrational features of hexagonal hydroxyapatite Ca₁₀(PO₄)₆(OH)₂. *Phys Chem Chem Phys* **2006**, *8* (21), 2464-2472.
7. (a) Broyden, C. G., The Convergence of a Class of Double-rank Minimization Algorithms 1. General Considerations. *IMA Journal of Applied Mathematics* **1970**, *6* (1), 76-90; (b) Broyden, C. G., The Convergence of a Class of Double-rank Minimization Algorithms: 2. The New Algorithm. *IMA Journal of Applied Mathematics* **1970**, *6* (3), 222-231; (c) Fletcher, R., A new approach to variable metric algorithms. *Computer Journal* **1970**, *13* (3), 317-&; (d) Goldfarb, D., A family of variable-metric methods derived by variational means. *Mathematics of Computation* **1970**, *24* (109), 23-&; (e) Shanno, D. F., Conditioning of quasi-newton methods for function minimization. *Mathematics of Computation* **1970**, *24* (111), 647-&.
8. Perger, W. F.; Criswell, J.; Civalleri, B.; Dovesi, R., Ab-initio calculation of elastic constants of crystalline systems with the CRYSTAL code. *Comput Phys Commun* **2009**, *180* (10), 1753-1759.
9. Dovesi, R.; Orlando, R.; Erba, A.; Zicovich-Wilson, C. M.; Civalleri, B.; Casassa, S.; Maschio, L.; Ferrabone, M.; De La Pierre, M.; D'Arco, P.; Noël, Y.; Causà, M.; Rérat, M.; Kirtman, B., CRYSTAL14: A program for the ab initio investigation of crystalline solids. *Int J Quantum Chem* **2014**, *114* (19), 1287-1317.
10. Guillerme, V.; Ragon, F.; Dan-Hardi, M.; Devic, T.; Vishnuvarthan, M.; Campo, B.; Vimont, A.; Clet, G.; Yang, Q.; Maurin, G.; Férey, G.; Vittadini, A.; Gross, S.; Serre, C., A series of isorecticular, highly stable, porous zirconium oxide based metal-organic frameworks. *Angew Chem Int Ed* **2012**, *51* (37), 9267-71.
11. Ortiz, A. U.; Boutin, A.; Fuchs, A. H.; Coudert, F.-X., Metal-organic frameworks with wine-rack motif: What determines their flexibility and elastic properties? *J Chem Phys* **2013**, *138* (17).
12. Lethbridge, Z. A. D.; Walton, R. I.; Marmier, A. S. H.; Smith, C. W.; Evans, K. E., Elastic anisotropy and extreme Poisson's ratios in single crystals. *Acta Mater* **2010**, *58* (19), 6444-6451.
13. Tan, J. C.; Civalleri, B.; Lin, C. C.; Valenzano, L.; Galvelis, R.; Chen, P. F.; Bennett, T. D.; Mellot-Draznieks, C.; Zicovich-Wilson, C. M.; Cheetham, A. K., Exceptionally Low Shear Modulus in a Prototypical Imidazole-Based Metal-Organic Framework. *Phys Rev Lett* **2012**, *108* (9), 095502.
14. Bahr, D. F.; Reid, J. A.; Mook, W. M.; Bauer, C. A.; Stumpf, R.; Skulan, A. J.; Moody, N. R.; Simmons, B. A.; Shindel, M. M.; Allendorf, M. D., Mechanical properties of cubic zinc carboxylate IRMOF-1 metal-organic framework crystals. *Phys Rev B* **2007**, *76* (18).